# REPORT DOCUMENTATION PAGE

Form Approved
OMB NO. 0704-0188



| 1. AGENCY USE ONLY ( Leave Blank) | 2. REPORT DATE | 3. REPORT TYPE AND DATES COVERED |
|---|---|---|
| | 28-Dec-98 | Final Progress Report |

4. TITLE AND SUBTITLE
Elucidation of the Fundamental Mechanisms of Diamond Film Growth

5. FUNDING NUMBERS
DAAH04-94-G-0326

6. AUTHOR(S)
Rik Blumenthal

7. PERFORMING ORGANIZATION NAME(S) AND ADDRESS(ES)
Auburn University
305 Samford Hall
Auburn, AL 36849

8. PERFORMING ORGANIZATION REPORT NUMBER
Army-Blumenthal-Final-98

9. SPONSORING / MONITORING AGENCY NAME(S) AND ADDRESS(ES)
U. S. Army Research Office
P.O. Box 12211
Research Triangle Park, NC 27709-2211

10. SPONSORING / MONITORING AGENCY REPORT NUMBER
ARO 33520.7-PH-DPS

11. SUPPLEMENTARY NOTES
The views, opinions and/or findings contained in this report are those of the author(s) and should not be construed as an official Department of the Army position, policy or decision, unless so designated by other documentation.

12 a. DISTRIBUTION / AVAILABILITY STATEMENT
Approved for public release: distribution unlimited.

12 b. DISTRIBUTION CODE

13. ABSTRACT (Maximum 200 words)

A new probe of high-density plasmas has been developed. Supersonic pulse, plasma sampling mass spectrometry has been shown to be capable of obtaining a "snapshot" of the chemical composition of a plasma. The technique is based on the release of a short pulse of noble gas into the near vacuum. As the pulse expands, the molecular and atomic species present in the plasma are swept into the rapidly expanding noble gas pulse. If the pulse is sufficiently dense, the gas mixture will supercool and condense with the plasma species acting as the nucleation sites for cluster formation. Contained within noble gas clusters, the plasma species are transported from the plasma chamber and to the detector with no significant chance of reaction or decomposition. This new method has provided strong evidence that the "growth species" for diamond is the vinyl radical (C2H3), and the chemistry of these plasmas has been shown to be parallel combustion chemistry. Application of this new method during the etching of silicon has provided the first mass spectrometric evidence for the highly dissociated chlorine, predicted by modeling. In addition, this method has been used to determine the direct etch products of Si, GaAs and AlN.

14. SUBJECT TERMS
Plasma; Mass spectrometry; Diamond; Semiconductors; Silicon; Gallium Arsenide
Aluminum nitride; Gas Expansion; Supercooling; Radicals

15. NUMBER OF PAGES
29

16. PRICE CODE

| 17. SECURITY CLASSIFICATION OR REPORT | 18. SECURITY CLASSIFICATION ON THIS PAGE | 19. SECURITY CLASSIFICATION OF ABSTRACT | 20. LIMITATION OF ABSTRACT |
|---|---|---|---|
| UNCLASSIFIED | UNCLASSIFIED | UNCLASSIFIED | UL |

NSN 7540-01-280-5500

Standard Form 298 (Rev.2-89)
Prescribed by ANSI Std. 239-18
298-102

2. Table of Contents

3. List of Figures

4. Statement of Problem Studied

There were several well-defined goals for this project. While the theme of the project was to understand the fundamental chemical processes of diamond film deposition, the initial goal was to develop a new probe of plasma environments, know as supersonic plasma sampling mass spectrometry, that would be capable of making the reliable measurements of the chemical composition necessary to understand the chemistry of the plasmas used to deposit diamond films. Once developed, this new technique was used to investigate why diamond deposition depends only the carbon to hydrogen ratio, and not the chemical nature of the hydrocarbon feed used in the process. The conclusion of that phase of the work was that a fast interconversion of species results in similar chemical compositions over the $C_2H_2$-$C_2H_4$ mass range in most of the plasmas studied. The few remaining inconsistencies in the early results led to the use of isotopic labeling to differentiate between unreactive species and species that undergo closed cycle reaction sequences. The results of the isotopic studies confirmed the conclusions of the earlier work and revealed that molecular species in high-density plasmas have only a few reactive collisions. Expanding the use of this new technique to the etching of semiconductors, the direct etch products of silicon, GaAs and AlN etching with chlorine were determined, and the first mass spectrometric evidence for the high degree of dissociation predicted by modeling were obtained.

## 5.A. Investigating The Chemical Composition Of Plasma Environments

### 5.A.1. Background

Industrial plasmas are probably the most difficult environments to fully understand. Their innate complexity arises from their non-thermal nature. The major consequence of the non-thermal nature of these plasmas is that no direct correlation may exist between any two seemingly related properties of the plasma, such as the kinetic energy distributions of the ions and their negative counterparts, the electrons. Despite their complexity, non-thermal plasmas have become an integral component in modern materials and semiconductor processing. Consequently, significant efforts have been committed toward understanding these complex systems, specifically as they relate to the deposition and etching of thin films.

To completely characterize a non-thermal plasma process, one would have to measure many of the properties of the plasma simultaneously. Furthermore, to relate the process to some desired, or undesired, surface modification, one would have to make the measurements, *in-situ*, or during materials processing. Unfortunately, no single probe of the plasma environment is capable of obtaining the many different measurements of plasma properties necessary to completely characterize the plasma. Every plasma diagnostic has its individual strengths and weaknesses that enable it to accurately measure one or more properties, while limiting its usefulness in addressing other properties. Over the years, an impressive array of techniques have been used to probe plasma environments, including optical, electronic and mass spectrometric methods.

### 5.A.2. Optical Probes Of Plasmas

Optical probes of plasma environments have been reviewed recently,[1] and are capable of providing a wealth of information about a plasma. Viewed simply, optical methods can be divided into two distinct classifications, passive and active probes.

In optical emission, a passive spectroscopy, the light emitted from the plasma is detected and the intensity of specific emission lines, corresponding to discreet transitions from excited states to lower lying levels, are used to determine the relative, or in some cases the absolute, concentrations of specific species within the plasma. Optical emission is by far the most common in-situ diagnostic in use in industry today, and is capable of detecting the presence of any atomic or molecular species capable of emitting light in the plasma. However, as with all methods, optical emission has two important limitations. The first limitation arises from the broadening of the sharp atomic lines traditionally associated with atomic emission spectroscopy into broad bands in molecules. Typically, atomic emission spectra display 10-50 sharp lines corresponding to direct transitions between a few accessible electronic energy levels. In molecules, the vibrational and rotational energy levels are superimposed on each electronic state, resulting in the single line for each electronic transition being replaced with hundreds of individual lines corresponding to transitions between different combinations of vibrational and rotational excitations. These many lines may be experimentally unresolvable, producing the broad featureless the spectra typical of polyatomic molecules.

An even greater limitation of this method, even when considering only small molecules, is that the light detected originates from the transition from an excited state to a lower level making it proportional the population of the excited species, and not the ground state or the

overall population of the species. A determination of the actual population of the excited state requires an independent measurement of the cross-section for the specific transition measured. In some cases, such as the emission of atoms and many diatomics, the cross-section of many transitions have has been previously measured, but when the species of interest is a radical, or some other unstable species, the exact cross-section may be experimentally difficult to measure directly. In either case, the determination of the concentration of the species can only be achieved by relating the observed population of the excited states to the ground state population. In an equilibrium situation, the excited state population may be related to the ground state population directly through the temperature, using the Boltzmann relation:

$$P_{excited} / P_{ground} = e^{-(E_{excited} - E_{ground})/kT} \qquad (1)$$

where $P_{excited}$ and $P_{ground}$ are the probablities that a molecule or atom will be found in the excited or ground state, $E_{excited}$ and $E_{ground}$ are the energies of the excited and ground states, k is the Boltzmann constant, and T is the temperature. However, in the a non-equilibrium environment of a plasma, this relation is not valid.

Instead, the populations of the excited states must be determined from the probabilties for excitation by collisions of low energy electrons with the ground state molecules or atoms. To achieve this goal, it is often convienient to add trace amounts of noble gases to the plasma, to get an internal measure of the electron energy distribution. Relating the intensity of the emission line of interest to the intensity of a noble gas emission with the same excited state energy allows one to obtain the overall concentration of the species relative to the noble gas concentration. This method is known as actinometry, and is extremely useful where it can be applied. However, it is not practical were addition of noble gases is not acceptable or where the cross-sections for excitation are not known or readily measured.

Laser induced fluorscence is the most powerful active optical spectroscopy for the study of plasmas. In this method, laser light is tuned to a specific transition of the molecule to be studied and light emitted is detected. This method has two advantages of simple emission spectroscopy. Assuming that the appropriate cross-sections are known or may be measured, the signal is proportional to the number of molecules in the inital state By choosing the excitation properly, the population of both the ground state and the excited states may be determined. The second advatntage is the species selectivity which comes with the narrow band width laser light that excites only the specific excitation of interest in the specific molecule of interest. The disadvatages of this technique are similar to those encountered in optical emission. As one considers poly-atomic species, excitation lines like emission lines broaden into bands and species selectivity may be comprimised.

Optical absorption spectroscopies are very difficult in plasmas, primarily due to the large background emission noted above. Despite the difficulty of measuring a small loss of signal in the presence of an intense background, simple absorption measurements in the infrared has been able to determine the concentration of methyl radicals in diamond plasmas. Once again, the weakness of this method is that the vibrational absorption bands, like the optical cross-sections may not be know for radical and other reactive species found in plasmas.

5.A.3. Mass Spectrometric Methods

Mass spectrometry is a less common but certainly not unusual plasma probe. Downstream mass spectrometry is used as a plasma diagnostic in process control techniques. In these experiments, a mass spectrometer samples a fraction of the downstream flow through an aperture isolating the differentially pumped mass spectrometer from the higher pressure of the gas flow. Changes in the composition of the gas flow are used to monitor and detect changes in the process chamber. What is generally observed in these downstream experiments are a combination of reactants and fully formed molecular products of the process, such as $SiCl_4$, $AsCl_3$ and $GaCl_3$ in the case of semiconductor etching. The main advantage of mass spectrometry over optical methods is its ability to discriminate between and simultaneously measure wide ranges of polyatomic species. Its main weakness is the low pressure operating environment necessary for the detector ($\sim 10^{-6}$ Torr) which requires the use differential pumping and gas sampling.

Measurement of the "actual" composition of the gas in the plasma is inhibited by the low-pressure necessary for mass spectrometry. Attempts to overcome this limitation have included the development of molecular beam mass spectrometry[2,3] and the supersonic pulse, plasma sampling method described in depth below. Molecular beam mass spectrometry is distinguished form other aperture sampling methods by the precise choice of aperture size and shape which ensure free expansion of the gas at the detector side the aperture. In many cases, the aperture may be an ion milled channel through the sample wafer,[2] in other cases it may be a skimmer or aperture placed into the gas flow very near the processing chamber. In either case, the sample of gas detected traverses a region, albeit a short one, at processing pressures out the electric and magnetic fields characteristic of the plasma region and in close proximity to surfaces of the wafer or the skimmer where recombination and surface reactions cannot be ignored.

Mass spectrometric detectors of ions in the plasma environment have been recently commercially marketed.[4] Although this method does provide the capability to detect and distinguish molecular ion in the plasma, there is not guarantee that the distribution of ionic species (approximately one part in 1,000,000 in a high density plasma) accurately reflects the distribution of neutral species in the non-equilibrium environment of the plasma.

Supersonic pulse, plasma sampling mass spectrometry is capable of collecting and detecting a sample of the atomic and molecular constituents of the low-pressure plasma environment. Greatly simplified, a pulse of noble gas is released into the plasma environment above the surface of the wafer. As the pulse supersonically expands, it cools. If the pulse has sufficient initial density, the gas will supercool well beyond the normal condensation temperature at the pressure of the process chamber. Molecular and atomic species originally in the plasma region are swept into the expanding noble gas pulse by collisions with the much higher-pressure noble gas atoms. As the temperature of the gas mixture, noble gas and plasma sample, cluster formation begins with the plasma sample species acting as nucleation site for initial cluster formation. Once the cluster formation has begun in the supercooled environment, clustering continues until all of the gas is consumed and the expansion ceases. The pulse, comprised of clusters, continues along its original path to the detector. The result of this process is that the plasma sampled species are preferentially incorporated into the center of noble gas clusters, which protect them against reaction during transport to the mass spectrometer. One might say that the plasma sample is argon matrix isolated in free space.

## 5.B Supersonic Pulse, Plasma Sampling Mass Spectroscopy

Supersonic pulse, plasma sampling mass spectra was designed to probe the chemical composition of low-pressure environments, specifically plasmas. The goal of the technique is to remove reactive species from the plasma with the minimum possibility of perturbing the chemical nature of the species before detection. The experimental method is based on the release a pulse of noble gas into a low-pressure environment. Upon expansion, the center of the pulse will cool, and possibly condense, as it passes through the region of the plasma. Molecular species, including radicals, originally part of the plasma are swept along with the pulse and arrive at the detector at the same time as the noble gas pulse. In the incorporation process, the only interactions that will occur are near-thermal energy collisions with the far more numerous noble gas atoms of the pulse.

No description or discussion of the capabilities and limitations of this new mass spectrometric method can be complete without a detailed description of the pulsed supersonic, sampling method that distinguishes it from other mass spectrometric methods. It is the incorporation method that makes this new technique uniquely capable of detecting the actual chemical composition within plasma. Time-of-flight analysis of the velocity distributions of both the species incorporated within the pulse and the noble gas itself have been used to investigate the physical processes responsible for the incorporation of plasma-born species into the pulse.

### 5.B.1 Free Expansions From Apertures

The theoretical basis for supersonic expansion of ideal gases from nozzle sources is well established.[5] Essentially, gas flows out of a stagnation volume through an aperture and expands isentropically into a region of lower pressure. Isentropic expansion continues until the "sudden freeze" point, when the gas density falls below the maximum density for molecular gas flow. From that point forward, the expansion can be viewed as "collisionless" molecular flow. During the isentropic expansion, the latent heat of the gas at stagnation ($H_0$) is converted into kinetic energy of the gas flow ($\frac{1}{2} mv_f^2$) while the gas in the center of flow velocity ($v_f$) coordinate system cools according to the energy conservation relation,

$$H_0 = H(T) + C_p(T_0-T) = H(T) + \tfrac{1}{2} mv_f^2, \qquad (2)$$

where $C_p$ is the heat capacity of the gas at constant pressure, $T_0$ is the temperature at stagnation, and T is the final temperature of the gas. Flow velocities exceeding the local speed of sound, supersonic expansions, are easily attained in free expansions. The gas density (N) during the isentropic expansion may be calculated as:

$$\frac{N}{N_o} = \left(1+\frac{(\gamma+1)}{2} M^2\right)^{1/(1-\gamma)}, \qquad (3)$$

where $N_0$ is the gas density at stagnation, $\gamma$ is the ratio of the heat capacity ratio $C_p/C_v$ (5/3 for an ideal monatomic gas), and M is the Mach number, defined as the flow velocity ($v_f$) divided by the speed of sound in the local environment.

Clustering of atoms in free expansions has also been discussed extensively in the literature.[6] However, the extremely complex interactions of the rapidly changing gas densities and pressures, coupled with the need to include the non-ideal behavior of real gases to explain the interatomic attractions necessary for clustering, has resulted in the development of no satisfactory theoretical treatments of this process.[6,7] Consequently, much of the understanding of these processes is drawn from the scaling of one set of experimental results with previous observations based upon the principle of corresponding states.

Although no complete theoretical foundation exists for clustering, it is important to consider both how and when clustering, or condensation, may occur. The phase diagram of argon is shown in Fig. 1.[8] The isentropic expansion of an ideal gas is shown as the line connecting our typical stagnation conditions with the point of sudden freeze. If as depicted, the line crosses the phase boundary between the gas and a condensed phase, the liquid, clustering should occur. When using Fig. 1 to understand the expansion of a real gas, it is important to note that movement along the line from the stagnation conditions to the "sudden freeze" can be interpreted as the time evolution, or path, of the system. For an ideal gas, removing heat from the system results in a linear decrease in temperature, which constrains the system to movement only along the line. For a real gas, removing heat also results in a decreasing temperature, but only until the temperature drops to the boiling point of the liquid, after which the temperature remains constant until condensation is complete. On the figure, the behavior of a real gas would also begin at the stagnation point and follow the line, but only until it crosses the phase boundary, at which time the path of the system would shift from the line and to the phase boundary, until clustering of the gas is complete, and there is no further gas to expand and cool the system.

### 5.B.2 Nucleation Theory And Clustering

Nucleation theory is also well established in the literature.[9] The salient issue to this discussion is how the increase in the free energy, arising from the high surface area to volume ratio of clusters and small droplets, effects the rate at which condensation occurs. In Volmer-Weber-Becker-Doering theory, the nucleation rate in supersaturated gases is taken as the density of critical nuclei times the rate of growth of the nuclei (which occurs through monomer additions only). The critical nuclei size is calculated from the maximum in free energy as function of cluster size, given by,

$$\Delta G_i = 4\pi r^2\sigma + \frac{4}{3}\pi r^3 \Delta G_v, \qquad (4)$$

where r is the radius of the cluster, $\sigma$ is the surface tension, and $\Delta G_v$ is the free energy of the bulk liquid , calculated as:

$$\Delta G_v = -(kT/\Omega)\ln(p/p_e), \qquad (5)$$

where $\Omega$ is the molecular volume of the gas, p is the real pressure and $p_e$ is the equilibrium pressure at temperature T. A plot of the free energy of argon as a function of cluster size is shown in Fig. 2 for several temperatures below the normal boiling point. The critical radius (r*), or the radius at the maximum of free energy, may be determined by setting the derivative of equation (4) equal to zero and solving for the radius, yielding,

$$r^* = -2\sigma / \Delta G_v . \qquad (6)$$

Below the critical radius, clusters are unstable and will tend to dissociate, while above the critical radius clusters will grow indefinitely. The free energy of the critical cluster may be calculated by substitution of the critical radius back into equation (4), to get a free energy for critical nuclei,

$$\Delta G^* = (16/3)\pi\sigma^3 / \Delta G_v . \qquad (7)$$

The concentration of critical nuclei may then be calculated from the monomeric gas density using a Boltzmann distribution of cluster size based on the free energy of cluster formation

$$n^* = n_{monomer}\, e^{(-\Delta G^*/kT)}, \qquad (8)$$

where $n^*$ is the density of critical clusters, $n_{monomer}$ is the density of monomeric units, approximated as the total gas density, and $\Delta G^*$ is the free energy of formation of a critical cluster. Finally, the rate of nucleation (J) may be calculated as:

$$J = n^* \alpha \left[ \frac{P}{(2\pi mkT)^{1/2}} \right] \left(4\pi r^{*2}\right) \qquad (9)$$

where $\alpha$ is the accommodation coefficient and m is the mass of the monomer. The accommodation coefficient represents the probability of a monomer sticking to the cluster should a collision occur. The term in the brackets is the frequency of collisions of monomer per unit surface area, given by simple collision theory, and final term is the surface area of a critical cluster.

### 5.B.3 Continuous And Pulsed Release Of Real Gases

The continuous release of gas from a nozzle source has been previously described in detail.[7] Very simply, as the gas passes through the aperture flow becomes directionally oriented with a velocity equal to the speed of sound at stagnation. As the gas emerges from the aperture, it begins to expand both axially and radially. It is the axial component of the expansion that is responsible for the acceleration of the gas to supersonic speeds. The continuous expansion of the gas in the radial direction results in the establishment of an effective pressure gradient that extends from the axis of the supersonic beam to a point where the source gas pressure is equal to the background gas pressure, defining the boundary of the jet. Theoretical treatments of jets as isentropic expansions, described above, are based on expansions into a perfect vacuum, which cannot reflect shocks back at the jet. However, excellent agreement has been observed between this seemingly over-simplified model and experimental measurements, which are obtained with low, but not zero, background gas pressures. This high level of agreement is attributable to inability of the low-pressure background gas, or the shock waves reflected from it, to penetrate the pressure gradient that that extends from the axis of expansion. This effect is critical to understanding the differences between pulsed and continuous expansion. To reiterate, in continuous expansions, the radial expansion, or flow, of the source gas overwhelms the molecular flow of the background gas, virtually eliminating penetration of jet by the background gas.

In pulsed gas expansions, the situation is very different. To maintain adequate vacuum conditions for the expansion, the delay between the release of successive gas pulses must be sufficiently long for the source gas to be pumped from the chamber. As the source gas is being pumped, the background gas has more than sufficient time to re-establish a uniform density throughout the vacuum chamber, including the region directly in front of the aperture, or within the jet boundary. Upon opening of the valve, source gas will begin to expand into jet region, already containing background gas molecules. Collisions of the initially randomly moving background gas molecules with leading edge of the much more dense highly directional pulse will result in accommodation of the initial momentum background gas molecules into the pulse. Over distances of a few aperture radii, the density of the source gas will remain above the molecular flow limit, and the incorporation process may be pictured as an expanding viscous plug of source gas overtaking stationary background molecules.

### 5.B.4 Effect Of Gas Incorporation On The Expansion Of Real Gases

All of the observed effects of the background gas on the velocity distributions of a pulsed free expansion can be explained as the simple consequences of mixing on supercooling of the gas. A supercooled gas is meta-stable state, where the a specific phase may persist below the normal phase transition temperature. The origin of supercooling can be understood by following the time evolution of the gas pulse in terms of Fig. 1. Initially, the system (the gas pulse) is at rest and the conditions those of stagnation. When the valve is opened, the gas expands isentropically, moving along the line toward the phase boundary. At the point where the line crosses the phase boundary, thermodynamics would dictate that at the system cross over from the line to the phase boundary, as the expanding system continues to cool both the gas and condensed phases coexisting. However, if the system is moving rapidly, as it encounters the phase boundary, kinetics may dictate the behavior of the system. In this case, the system may continue to follow the line, beyond the phase boundary, for some period of time. The extension of the gas-like behavior, or isentropic expansion, into the liquid and solid phase regions is know as supercooling. All isentropic expansions are by nature extremely fast processes, and therefore, supercooling is always observed in free expansions.

Evidence of supercooling can be seen in the most probable velocities of Fig. 3, which shows the velocity distributions as a function of methane gas pressure in the plasma chamber. Pulses released into pressures $<1x10^{-7}$ Torr have a most probable kinetic energy ($\frac{1}{2}mv_f^2$) of 5940 J/mol. Using Eq. 2, and assuming a heat capacity of 5/2R for the argon, the experimentally measured kinetic energy indicates a temperature drop ($T_0$-T) of 286K. Beginning at the stagnation temperature of 298K, a final temperature of only 12K is obtained. However, the phase diagram of argon, Fig. 1, indicates that the gas should condense at the crossing point of the line and the phase boundary, at a temperature of 97.2K. The most reasonable explanation of this observation is that supercooling had occurred; the gas phase persisted beyond the phase boundary until 12K when condensation, or clustering, occurred.

The onset of clustering, or the endpoint of isentropic expansion, may be understood as occurring when the temperature has been lowered sufficiently for the kinetics of condensation to compete with the rate of gas expansion. Since the rate of expansion always remains fast, a competition between the processes can only exist when the rate of clustering becomes very fast. At temperatures only slightly below the normal boiling point, a significant free energy barrier to

condensation exists. As temperatures further below the normal boiling point are considered, the free energy barrier decreases as the barrier maximum, shifts to smaller critical cluster sizes, see Fig. 2. The point where condensation will certainly occur is at the temperature at which the maximum in free energy is only two atoms. At this temperature, the result of any collision is the formation of a stable cluster, for which continued growth is always energetically favored. Under these conditions, the number of gas phase species would proceed to halve in the average time between collisions, at a rate faster than isentropic expansion can occur. One very important point that must be made about Fig. 2. As plotted, the graph appears to indicate that supercooling by only ~30K might be sufficient to achieve a critical cluster size of two atoms. However, it should be recalled that the curves shown were calculated using the infinite cluster size limit, or bulk values, of the surface and liquid-phase free energies. When considering clusters that are small, even less than even a few hundred atoms, the properties of the cluster cannot be taken as equal to those of the bulk liquid or solid. In other words, a plot of this type may be instructive in describing the physical mechanism of the nucleation, but should not be taken as being numerically accurate.

The fundamental effect of the incorporation of background gas into the pulse is to introduce the possibility of generating mixed clusters during the supercooling phase. Mixing of liquids is well understood,[10] and introduces an extra free energy term that would be added to the two original terms in Eq. 4. In its simplest form, the mixing of ideal liquids, the third term is written as,

$$\Delta G_{mix} = RT(\chi_A \ln \chi_A + \chi_B \ln \chi_B), \qquad (10)$$

where $\chi_A$ is the fraction of A molecules in the cluster and $\chi_B$ is the fraction of B molecules in the cluster. The ideal free energy of mixing term, shown in Eq. 10, is always negative, and consequently, a mixed cluster always has an energy below that of a pure cluster. Further, if the free energy of mixing is included, Eq. 8 becomes,

$$n^* = n_{monomer}\, e^{-(\chi_A \ln \chi_A + \chi_B \ln \chi_B)}\, e^{(-\Delta G^*/kT)} \qquad (11)$$

which predicts a concentration of critical clusters in the mixed system to be greater than the concentration of critical clusters in a pure gas. Carrying the higher concentration of critical nuclei into Eq. 9, an increase in the rate of nucleation can be predicted. It should be noted the ideal mixing effect results in an increase in the condensation rate of a factor of two when the critical cluster size is two. However, the influence of only one background gas molecule per cluster is significant to much larger cluster sizes. For example, at a critical cluster size of thirty, the rate of condensation will be over twenty percent faster than would be observed in the pure gas. To summarize, mixing lowers the free energy of each cluster, which translates into a lower barrier to condensation, which in turn translates into an acceleration the kinetics of condensation.

### 5.B.5 Sampling Volume in Supersonic Pulse, Plasma Sampling Mass Spectrometry

The effective volume of the plasma chamber probed by this technique may be assumed to be a cylindrical region, with a diameter defined by the aperture, extending out from the pulsed valve to the distance where the gas density falls below the molecular flow limit. Beyond this point, the pulse may be treated as a molecular flow fluid, passing through any other molecular flow fluid with negligible interactions. Consequently, the distance at which molecular flow is

achieved may be determined by measuring extra path length necessary for a reflected fraction of the shock-front to pass through the direct flow without interfering with the direct flow. A measurement of this nature can be accomplished by placing a silicon wafer (~ two-inches by two-inches) on the sample holder and raising the wafer until the direct beam is almost blocked. The vertical height of the sample may then be varied and the time-of flight distributions of the argon pulse measured as a function of the vertical height of the surface as it is incrementally lowered, see Fig 4. The data in the figure are shown in 0.20" steps, up to a maximum distance of 1.00" for presentation purposes, although the time-of-flight spectra were collected in 0.05" steps. Placement of the sample surface at distances greater than 0.75" below the direct beam path resulted in spectra which were indistinguishable from spectra with the sample retracted > 1.5-inches. At sample heights between 0.70 and 0.55 inches below the direct path, the spectra show a reduced maximum height and distinct shoulder at the fastest flight-times, appearing almost identical to the spectra taken at 0.60" below the direct path. With the sample placed 0.10 to 0.50 inches below the direct path, a double peaked spectrum is observed which only slowly decreases in intensity as distance between the sample and the direct beam is decreased. At 0.05-inches below the direct beam the signal drops precipitously until essentially no signal is observed at 0.00-inches, as seen in Fig. 4.

The data indicate that the interactions of the direct and scattered pulses can be observed to begin at a sample height of 0.70-inches, with a much more significant interaction occurring at a height of 0.50-inches. Assuming the maximum extra path length traveled by the reflected pulse is 1.40 inches with a 550 m/s velocity, one can calculate that the reflected pulse will cross the direct path only 65 ms after the direct pulse. Considering the order of magnitude larger temporal widths of all of the spectra measured, it must be concluded that in all cases, the reflected pulse will pass through, and not simply behind, the direct pulse. Overall, the two distinct regimes of the time-of-flight spectra may be interpreted as follows. At distances greater than 0.70 inches, the crossing of the pulses must occur after the pressures in both pulses have achieved molecular flow conditions. Between 0.70 and 0.55 inches, the crossing occurs after the reflected pulse has reached the molecular flow limit, but before the direct pulse has reached the molecular flow limit. Between 0.50 and 0.10 inches, the significant scattering of the direct pulse indicate that the crossing of the two pulses occurs before either one has achieved molecular flow.

Using the 0.55 inch retraction as the limit where the reflected beam path is equal to the distance where molecular flow is achieved, it is possible to deduce the distance from a simple geometric arguments that take into account the ~2-inch length of the surface and its position with the its leading edge placed 0.25-inch downstream of the nozzle aperture. The results of such an analysis indicate the distance at which a pulse released into a vacuum achieves molecular flow is between 1.12 and 1.35 inches. Consequently, we conclude that the maximum sampling volume, expansion into the lowest pressures of gas, is approximately $6 \times 10^{-3}$ $cm^3$. Further experimental work probing the interactions of the direct and scattered pulses as a function of the pressure into which the pulse is released could be used to investigate the changes in the sampling volume induced by premature nucleation in the presence of the background gas.

### 5.B.6 Signal Levels And Noise Considerations

The methane mass spectrometric signal is shown in Fig. 5, plotted as the counts per pulse collected in a single time period. Assuming Poisson, or counting, statistics the calculation of the

both the signal and the noise of time of flight data are both straightforward. The signal in any channel will scale linearly with the number of pulses summed into the spectrum, and the noise will be the square root of the signal. The calculation of the signal and noise in a supersonic pulse, plasma sampling mass spectrum is also straightforward, but not as simple. As can be seen in Figure 5, non-zero baselines may exist for some species that may even vary with the pressure of a feed gas in the plasma chamber. The baselines are simply the result of a non-zero partial pressure of background gas in the UHV chamber contributing to the overall signal. In mass spectrometric measurements, a baseline count is measured once before and once after the arrival of the pulse in the UHV chamber, and the average is subtracted from the in-phase count to get the signal, or counts attributed to the gas pulse. Since the noise in the measurement is the square root of the total count, noise levels larger than the square root of the signal can be observed, particularly at m/e = 17, 18, and 28, corresponding to typical UHV contaminants $H_20$ and $N_2$/CO. In most cases, the baselines have been observed to remain constant throughout a series of experiments. However, in the worst case scenario, as depicted in Fig. 5, the mass of interest may be the same as the mass of a feed gas or a daughter ion of the feed gas. In these cases, the baseline may change as a function of the pressure of the feed gas in the plasma chamber. Analysis of the noise level in the data of Fig. 5 provides a useful example of real signal to noise behavior. From the figure one may observe that the counts attributable to the pulse saturate, remaining relatively constant between plasma chamber pressures between $2.6 \times 10^{-4}$ and $1.2 \times 10^{-3}$ Torr. Focussing of the data corresponding to the two limits, $2.6 \times 10^{-4}$ and $1.2 \times 10^{-3}$ Torr, the integrated counts under the peaks are found to be 32.14 and 24.89 counts per pulse, respectively, with background signal levels of 25.04 and 9.23 counts per channel, respectively. Correcting for the signal loss due to overhead of the time-of –flight data acquisition routine which does not exist in the mass spectral routine and assuming the typical data collection time of 1000μs, single pulse signals of 43.6 and 36.1 counts on top of backgrounds of 363 and 134 counts would be observed. The single pulse signal to noise ratios calculated from these numbers are 2.2 and 2.8, respectively. Typically, mass spectra are summed over 100 scans, or 100 pulses per mass channel, resulting in signal to noise ratios of 21.6 and 27.7, respectively for the two pressures. It should also be noted that the higher limits of plasma chamber pressure, the methane partial pressure in the UHV chamber was observed to build-up to as high as $1 \times 10^{-8}$ Torr, considerably higher than partial pressure of the normal UHV contaminant peaks. It may then be concluded that in the absence of background gas interferences, such as the measurement of chlorine atom (m/e =35) intensity, the noise in a measurement is very near the square root of the signal. While in the worst case scenario, signal to noise ratios of greater than 20:1 may be obtained with $\leq$100 pulse averaging. Finally, it is useful to note that it takes ~33 1/3 minutes to obtain a 100 pulse averaged 20.0 AMU wide mass spectrum at the typical 10 Hz pulse rate.

### 5.B.7 Summary of the Supersonic Pulse, Plasma Sampling Mass Spectrometry

The distinguishing characteristic of this technique is the sampling method, in which species originally in the plasma are incorporated into a short pulse of argon gas. To understand the process of gas incorporation into the pulse, we have measured the time-of-flight mass spectrometric signals corresponding to atoms, dimers and incorporated species for free expansions of argon. Interpretation of these spectra is based on including a free energy of gas mixing into the traditional treatment of a free expansion as isentropic. Including a free energy of mixing term into the energetics of nucleation results in a lowering of the free energy of barrier

and, thus, an increase in the kinetics of nucleation. Consequently, as the pressure of the background gas is increased, the expansion is terminated at earlier times, with less conversion of enthalpy to kinetic energy. In addition, the narrowing of the distribution is also observed as the background gas pressure is increased, which is not interpreted as a decrease in temperature, but as an increase in cluster size that accompanies nucleation earlier in the noble gas expansion process. Finally above a threshold pressure (~$10^{-4}$ Torr), all of the effects of gas mixing are seen to level off as one background gas molecule becomes available for the formation each critical nuclei. Overall, it can be concluded that the process of incorporation of molecular species into noble gas pulse is as nucleation sites for condensation of the noble gas of the pulse. The incorporated species are then transported to the detector isolated from one another and protected from reaction within clusters of noble gas atoms.

## 5.C Investigations of the Chemistry of Diamond Film Deposition

Investigation of the chemical processes of diamond film formation has been accomplished using several approaches. In the first work using supersonic pulse, plasma sampling mass spectrometry, the chemical compositions of 4% carbon in hydrogen plasmas based on different hydrocarbon feed gases were measured to access the extent or reaction and interconversion of the hydrocarbon species. In the second set of experiments, the reactivities of each hydrocarbon species was investigated using isotopic labeling of the hydrogen feed gas of the plasma. In addition, preliminary investigations of the chemical composition of the same plasmas have been carried out to examine the changes in the gas phase chemistry that accompany the actual deposition of diamond films.

### 5.C.1 Investigation Of The Composition Of 4% Carbon In Hydrogen Plasmas

The motivation for this work was to investigate why diamond deposition occurred in the same region of the carbon:hydrogen:oxygen ternary phase diagram, regardless of the chemical nature of the hydrocarbon used as the feed gas.[11] By determining the chemical compositions of 4% carbon-hydrogen plasmas with different carbon source feed gases, the species common to all the plasmas could be determined. The results of this study have been reported previously.[12] For the purposes of this summary, it is sufficient to note that when methane ($CH_4$) and ethane ($C_2H_6$) are used as the feed gases significant fractions of the feed gases remain unreacted, while roughly equal amounts of ethylene ($C_2H_4$) and acetylene ($C_2H_2$) are produced in the plasma. With ethylene as the feed gas, once again, equal amounts of ethylene and acetylene are observed to exist in the plasma. With acetylene as the feed gas, only a small percentage of ethylene is observed in the plasma.[13] Several important conclusions can be drawn from these results. First, since ethane and methane are only observed at significant concentration when they are the feed gases, they are not products of any chemistry common to all of the plasmas. In fact, the absence of significant amounts of methane in three out of the four plasmas is strong evidence against the premise that the methyl radical is the reactive species responsible for diamond film growth. Second, the presence of ethylene and acetylene in all of the plasmas indicates that these species are the common products of the plasma chemistry, and their roughly equal amounts (in three of the four plasmas) indicates that the two species are rapidly interconverting in the plasma environment, possibly indicating that one of these two species or more likely intermediate between them the vinyl radical ($C_2H_3$) is the growth species for diamond films.

## 5.C.2 Isotopic Labeling Studies Of 4% Carbon In Hydrogen Plasmas

### 5.C.2.a Acetylene In Hydrogen/Deuterium Plasmas

The only obvious inconsistency in the arguments above is the unequal proportions of ethylene and acetylene in the acetylene based plasma. Two possible explanations could be posed to explain this phenomena. The first explanation is that the acetylene feed gas is for thermodynamic, or some other reason, relatively unreactive. The other explanation is that the reaction pathway, in general, goes through ethylene on the way to forming acetylene, and the ethylene observed in the other plasmas is really the fraction of the hydrocarbons that were not able to react all the way to acetylene during their limited residence times in the plasma. Under this supposition, acetylene may react to form other species, but in the end, those species react to re-form acetylene.

A simple way to distinguish between these two possible explanations is to isotopically label the hydrogen gas in the plasma and detect the extent of isotopic labeling in the hydrocarbons. In the former case (unreactive acetylene), no isotopic labeling should be anticipated. In the latter case, the hydrocarbon upon its initial reaction with the labeled hydrogen (deuterium) atoms of the plasma would either lose a hydrogen to generate an acetylene radical, or add a deuterium to generate a labeled vinyl radical. To re-form acetylene the acetylene radical would add a deuterium atom resulting in the formation of a singly labeled acetylene, which through further cycles of hydrogen (deuterium) abstraction and addition could generate doubly labeled acetylene. Re-forming acetylene from the labeled vinyl radical would require the abstraction of one of the two hydrogen atoms (as opposed to the deuterium atom) in the second reaction step. Further cycles of addition followed by abstraction would produce greater and greater extents of deuteration. Either way, isotopic labeling will accompany one of the closed cycle reactions of acetylene in the plasma. Although both "closed cycle reactions of acetylene result in deuteration, it is further suggested that the observation of the vinyl radical ($C_2H_3$) and absence of the acetylene radical ($C_2H$) suggest that it is the latter cycle, hydrogen/deuterium atom addition followed by hydrogen/deuterium atom abstraction which occurs in the plasma.

Experiments carried out on acetylene in deuterium plasmas[14] show significant extents of deuteration, with 46% of the acetylene being doubly deuterated and 28% being singly deuterated. This result clearly demonstrates that the acetylene in not unreactive, and, using a simple statistical model of deuterium atom addition and hydrogen (deuterium) atom abstraction, it is possible to show that the extent of deuteration observed in the experiment corresponds to approximately six to eight total reactive steps. This result has great significance in terms of high-density (low-pressure) plasma processing of surfaces. The small number of reactive steps clearly rules out the assumption of a local equilibrium of chemical species in these environments, suggesting the important prospect that high density plasmas (with highly non-equilibrium fluxes of reactive species) can be used to achieve surface modifications not possible in higher pressure processing.

5.C.2.b Ethylene In Hydrogen/Deuterium Plasmas

The significant result of the investigations of ethylene in hydrogen/deuterium plasmas[15] is that the only deuterated species observed in the experiments were acetylene and the vinyl radical. All of the ethylene in the plasma remained unlabeled. This result suggests that the process of deuteration (deuterium addition to the hydrocarbon) does not occur until after the hydrocarbon has been stripped of hydrogen down to acetylene. After formation the acetylene may undergo (and not ethylene observed in the plasma represents hydrocarbon species that are in the process of reacting to form acetylene, which after formation undergoes closed cycle reactions, described above, to yield the deuterated acetylene observed. It should also be noted that the extent of deuteration observed in the acetylenes of the ethylene plasma is less than the extent observed in the acetylene plasma. This result may be readily understood by considering that the residence times of the two hydrocarbons should be roughly equal, yielding the same average number of reactive collisions. When acetylene is the feed gas, all reactive collisions contribute to the closed cycle reactions responsible for deuteration. However, when ethylene as the feed gas, the first two reactive collisions result in the stripping of the hydrocarbon down to acetylene, leaving two fewer reactive steps to result in the deuteration of the resulting acetylene.

5.C.2.c Ethane In Hydrogen/Deuterium Plasmas

The isotopic substitution study of ethane plasmas proved the most insight into the chemistry of high-density hydrocarbon-hydrogen plasmas.[16] Analysis of the deuterium plasma results revealed that the most abundant hydrocarbon, ethane, remained entirely undeuterated, while both the ethylene and acetylene showed significant extents of deuteration.

The presence of deuterated ethylenes indicates that the chemistry of this plasma differs from those studied previously. A survey of the combustion chemistry literature[17] revealed one reaction:

$$C_2H_5 + H \rightarrow CH_3 + CH_3 . \qquad (1)$$

that is uniquely accessible to plasmas with ethane as the hydrocarbon feed gas and can effectively compete with the more conventional two-body abstraction reaction:

$$C_2H_5 + H \rightarrow C_2H_4 + H_2 . \qquad (2)$$

Reaction 1 is particularly important for two reasons. First, unlike most hydrogen atom additions, it is a two-body reaction. At the low pressures of the plasmas studied, its two-body nature allows it to compete with the Reaction 2, which is also two-body. The second factor weighing in this reaction is the stability of the methyl radicals, which are the products of the reaction. Without the unusual stability of the two methyl radicals formed this reaction would be significantly uphill and would not be expected to proceed. Upon formation, the methyl radicals (one of which is labeled in the deuterium plasma) can either combine with a deuterium atom in a three-body reaction to form a labeled methane or recombine with each other in the two-body reverse reaction to Reaction 1to form isotopically labeled ethane radical ($C_2H_4D$). Multiple cycles of

carbon-carbon bond cleavage and re-formation (before the stripping of hydrogen to yield an ethylene) would explain the presence of the deuterated ethylenes observed in the ethane plasma.

The ultimate significance of these results is that the chemistry in high-density plasmas has been shown to be consistent with the neutral chemical pathways observed in combustion, although the reactions clearly do not proceed as far toward completion as would be anticipated in higher pressure environments.

### 5.C.2.d Methane In Hydrogen/Deuterium Plasmas

The experimental work on the isotopic substitution studies of methane-hydrogen plasmas has been completed. However, due to the interferences of water and deuterated water in the m/z = 14 – 20 region of the spectrum, the analysis of the mass spectra obtained will require the use of kinetic simulations of the plasma chemistry. Currently, a program under development has been able to reproduce the isotope labeling results of the acetylene and ethylene plasmas. However, to date, no adequate simulations of the methane or ethane results have been achieved. Upon completion of the code the results of the methane plasma studies will be analyzed and published.

### 5.C.3 Studies Of Chemical Composition During Diamond Film Deposition

These studies have proved to be experimentally quite difficult. The major problem is that radiation from the hot substrate heats the pulsed gas nozzle swelling the components and sealing the valve into the shut position. Therefore only one experiment can be carried out in a day and little signal averaging is possible. The most significant result of these preliminary studies carried out to date can be seen in Fig. 6. When the 2% ethylene in hydrogen plasma is ignited over a 650C silicon substrate, the m/z = 28 signal is observed to disappear while the m/z = 26 and 27 signals do not drop significantly. The only reasonable explanation for the remaining intensity of m/z =27 is as the parent ion of the vinyl radical. In fact, a lower bound of 40% vinyl radical can be established from this one mass spectrum.

### 5.C.4 Summary Of Diamond Film Deposition Results

Based on the isotopic studies, a complete model of the chemistry of these high-density diamond plasmas may be constructed. Overall, all hydrocarbons are stripped by hydrogen atoms (generated in excess by the plasma) down to acetylene, where further reaction results in the formation of the vinyl radical and then the re-forming of acetylene. The only exception to this general scheme is that the reaction of the ethane radical ($C_2H_5$) may result in the cleavage of the carbon-carbon bond yielding two methyl radicals and coupling the $C_2H_X$ and $CH_X$ reaction manifolds.

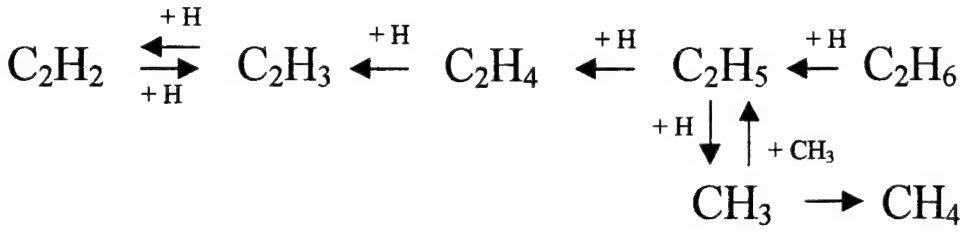


Scheme 1 - The mechanism of chemical reaction proposed for high-density hydrocarbon-hydrogen plasmas. Loss of molecular hydrogen and hydrogen atoms is neglected to simplify the notation.

Noting that diamond films may be grown from high-density plasmas using all of any of the hydrocarbons as the feed gas, it appears unlikely that is the "growth species" for diamond can be the methyl species, since it is not found in significant concentrations in three of the four systems studied. According to Scheme 1, it would appear that the most likely candidate for the "growth species" would be acetylene ($C_2H_2$) or the vinyl radical ($C_2H_3$) since they are the only species common to all of the plasmas from which diamond films may be deposited. The preliminary results of the "during growth" experiment tend to confirm this assignment.

## 5.D Investigations Of Semiconductor Etching

Considering the ability of supersonic pulse, plasma sampling mass spectrometry to detect reactive species and even determine their concentrations, the extension of this method into the study of the plasma etching of semiconductors seems quite natural. Despite being the backbone of semiconductor fabrication, little is known about the reactive species and direct products of semiconductor etching. Recently, supersonic pulse, plasma sampling mass spectrometry has been applied to the investigation of the percent dissociation of chlorine in during the etching of silicon, and the determination of the direct etch products of silicon, GaAs and III-V nitride etching.

### 5.D.1 The High-Density Plasma Etching Of Silicon With Chlorine

Details of the etch studies of silicon are described in the published reports.[18,19] Briefly, supersonic pulse, plasma sampling mass spectrometry has been used to investigate the percent decomposition of high density plasmas. At the same time industry has moved toward the use of high density plasmas , it has begun to rely more and more heavily on the simulation of plasma reactors for both reactor design and optimization of conditions for etching. However, the results of simulations and experimental studies of high-density plasma differed greatly, even when considering the most fundamental and critical property of an etch plasma: the degree of dissociation. Simulations of high-density plasmas indicated that under the proper conditions the chlorine would be >90% dissociated. Experimental evidence, gleaned from emission studies, appeared to confirm this conclusion, however, mass spectral evidence, considered a far more reliable measurement of actual species densities indicated the chlorine was only <30%

dissociated. Using supersonic pulse, plasma sampling mass spectrometry, the percent dissociation of the chlorine was measured in an ECR-microwave plasma as the pressure of the chlorine was varied. The results of these investigations showed that the percent dissociation of chlorine in the plasma varied from ~20-30% at higher pressures to over 85% dissociation at the lowest pressures. This study proved to be the first mass spectrometric confirmation of this important prediction of the simulation studies.

Supersonic pulse plasma sampling mass spectroscopy has also been applied to determine the direct etch product of ECR-microwave etching. To determine the identities of etch products and reactants, it is necessary to observe an increase or decrease, respectively, in concentration as the rate of etching is increased or decreased. By subtracting the mass spectrum obtained with the microwave power off from one obtained immediately after with the plasma ignited, two peaks are clearly observed to increase (m/z = 63 and 65, corresponding to $^{28}Si^{35}Cl$ and $^{28}Si^{37}Cl$) while the peak corresponding to $^{35}Cl_2$ (at m/z = 70) is observed to decrease. Similar experiments over additional mass ranges reveal m/z = 72 and 74 ($^{35}Cl^{35}Cl$ and $^{35}Cl^{35}Cl$) to behave identically to m/z = 70 and indicate no other peaks showing an increase. This data combined with the previous study clearly indicate that the plasma dissociates the chlorine into atoms, which react with the surface to yield a SiCl gas phase product.

### 5.D.2 The High-Density Plasma Etching Of GaAs And III-V Nitrides With Chlorine

The etch studies of GaAs and other III-V nitrides remain quite preliminary, however several important preliminary observations are worth noting. The direct etch products of GaAs have been studied in some detail. Mass spectra taken before and after ignition of the plasma are shown in Fig. 6. However, the continuous "dc" etching of GaAs with $Cl_2$ gas (a reaction which is not spontaneous in the case of Si etching) makes it difficult to interpret some of the data, as the "dc" etch products tend to build-up on the chamber walls only to be etched later by the plasma. The results of the gas etching of GaAs have been consistent with previous work, with the primary products being GaCl, $GaCl_2$ and $AsCl_3$. Ignition of a plasma has the effect of increasing the AsCl and $AsCl_2$ signals, while leaving the other signals peaks relatively constant.

The etching of AlN does not proceed spontaneously in $Cl_2$ gas making the interpretation of the data much easier. The mass spectra shown in Fig. 7 reveals the nitrogen containing etch products of a III-V nitride to be NCl and N atoms. $AlCl_2$ and to a lesser extent $NCl_2$ are also observed when etching. Currently, these experiments and additional investigations of GaN etching are being repeated and prepared for publication.

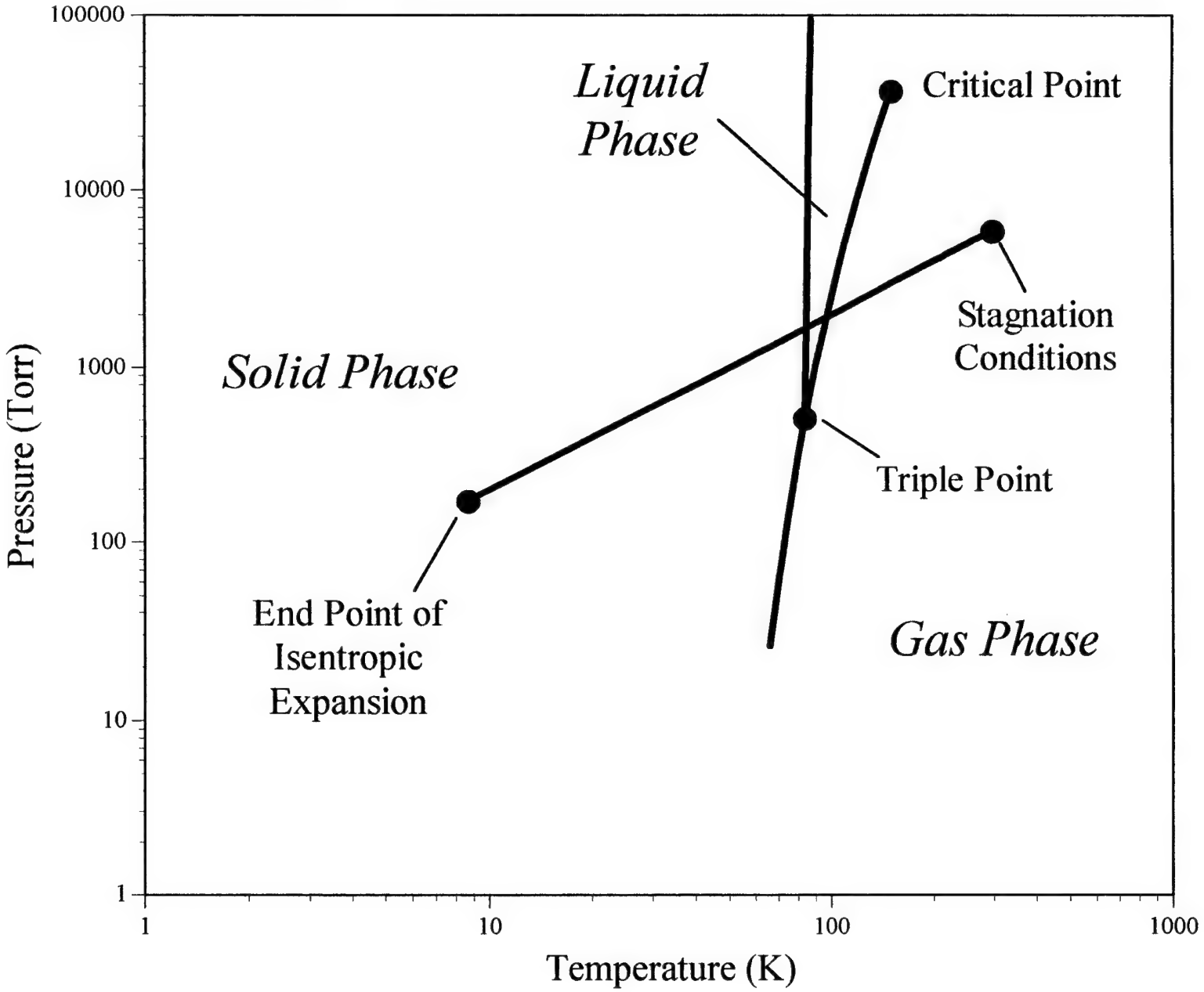


Figure 1 - The phase diagram of argon showing the evolution of the argon gas pulse from stagnation to the endpoint of isentropic expansion.

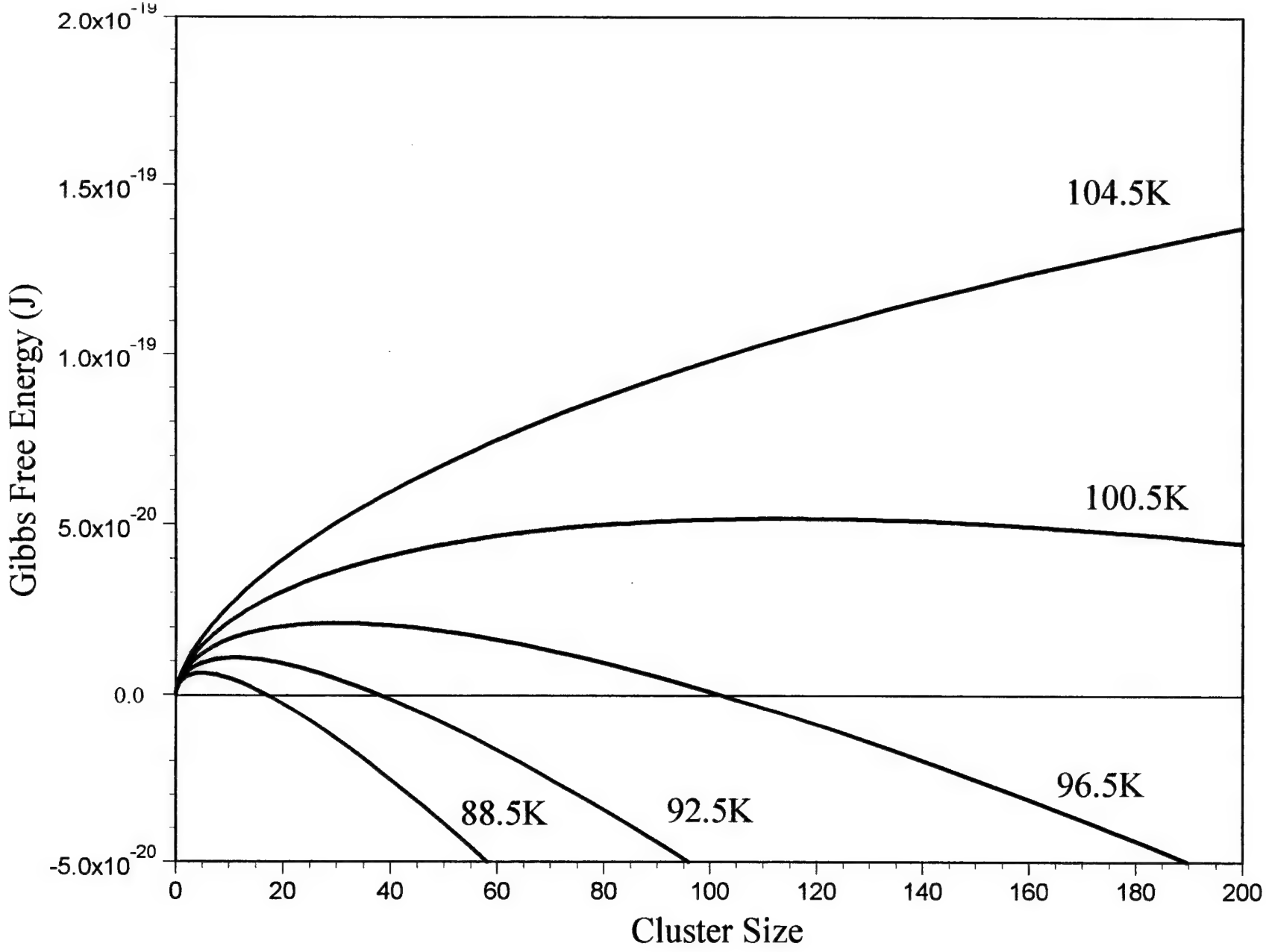


Figure 2 - The free energy of cluster formation as a function of argon cluster size for various temperatures below the condensation point.

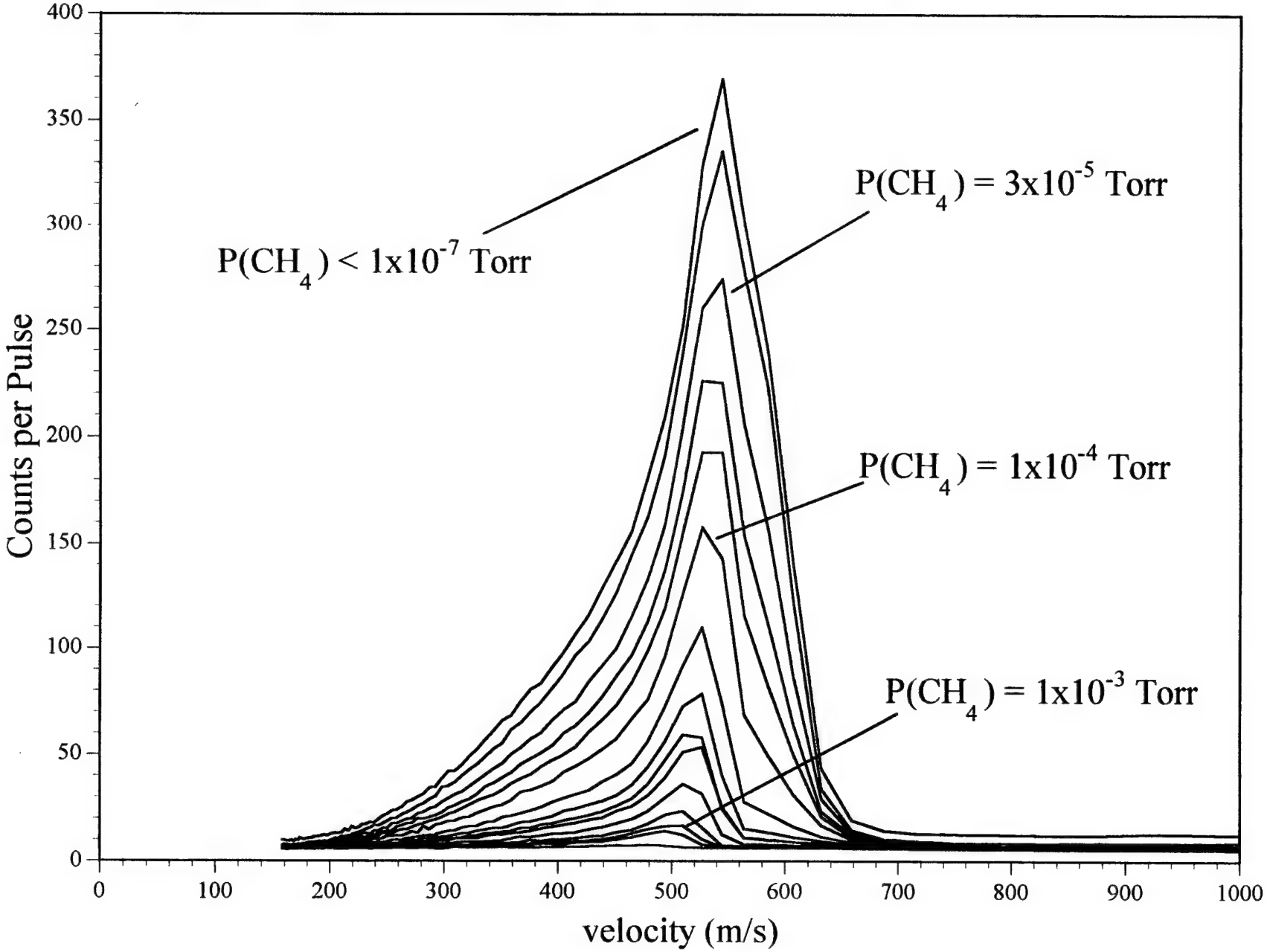


Figure 3 - Velocity distribution of argon monomer ion signal for 400μs argon pulses released into different pressures of methane gas.

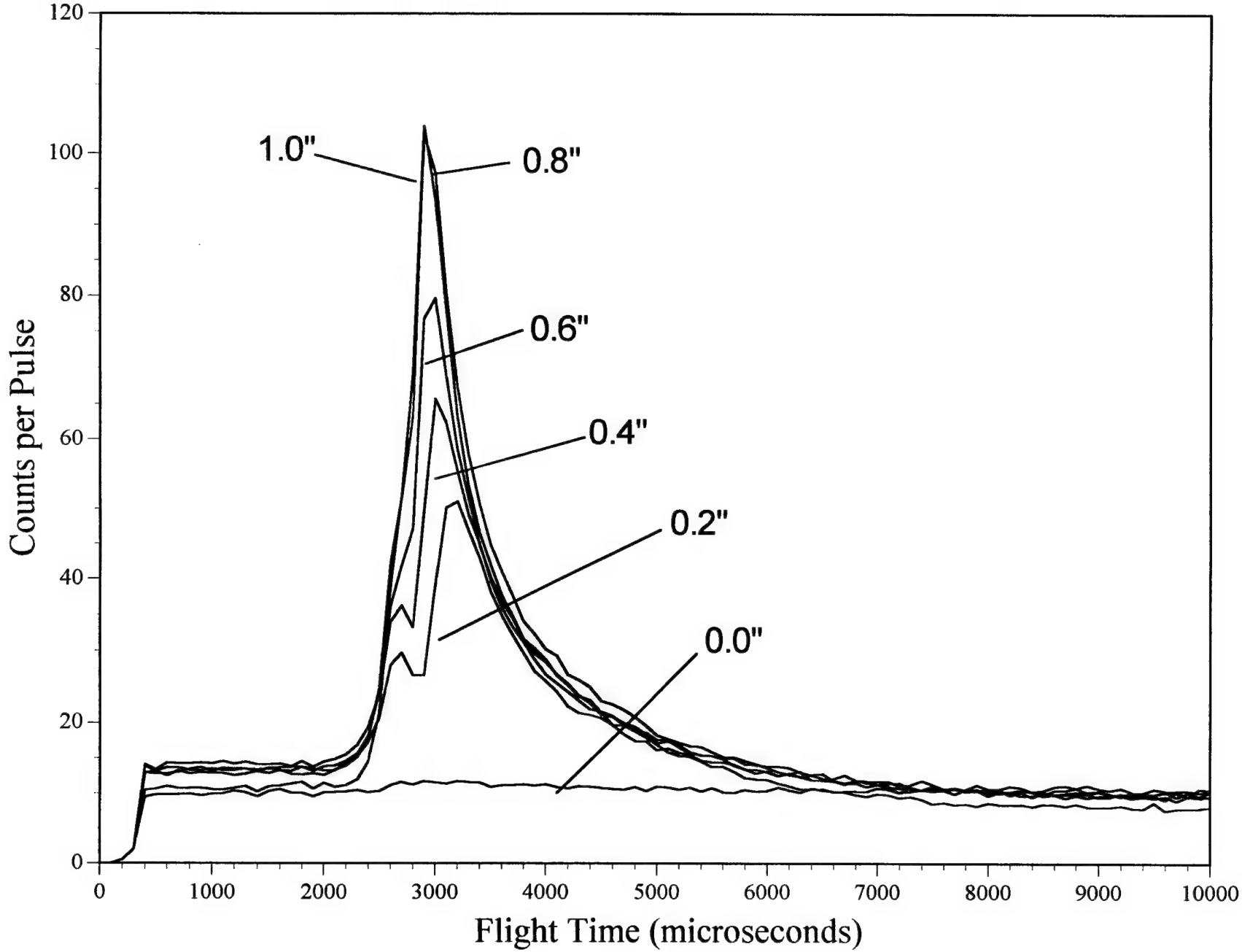


Figure 4 - Argon monomer ion signal as a function of flight time, shown as a function of sample height.

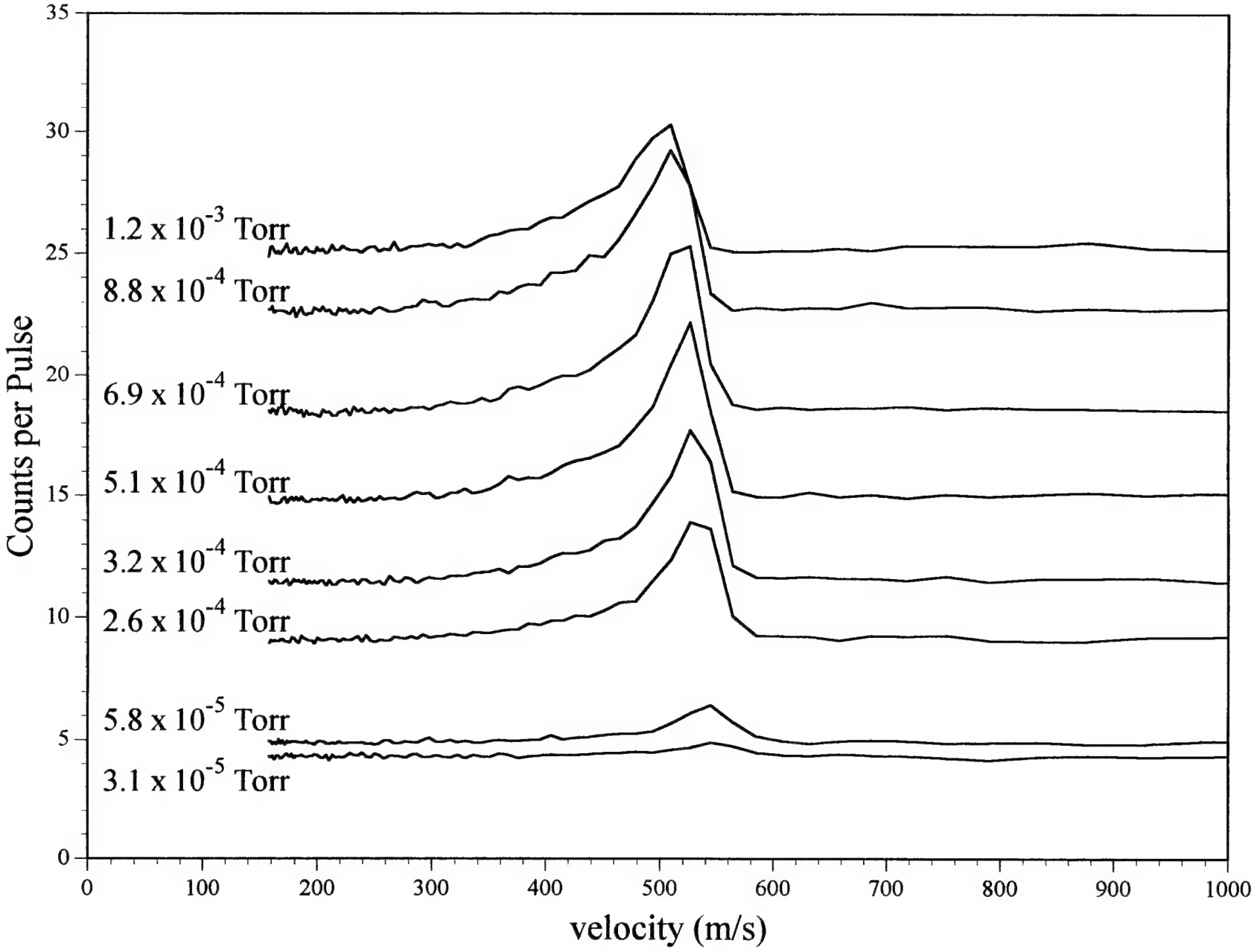


Figure 5 - Methane parent ion signal as a function of flight time shown for 400 μs argon pulses released into various pressures of methane.

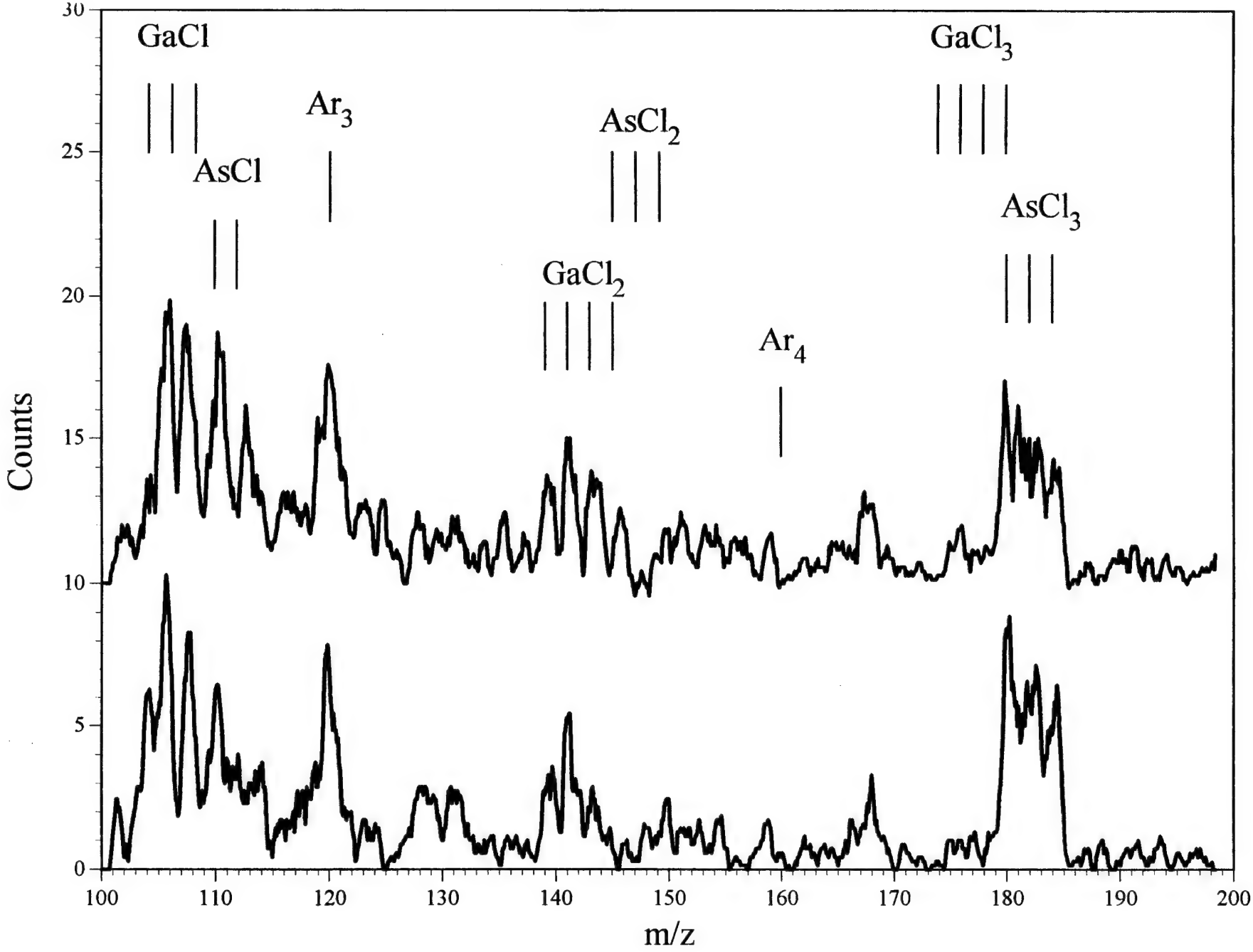


Figure 6 - Supersonic pulse, plasma sampling mass spectra obtained before ignition of chlorine plasma (below) and during the ECR-microwave plasma etching of a gallium arenside wafer (above).

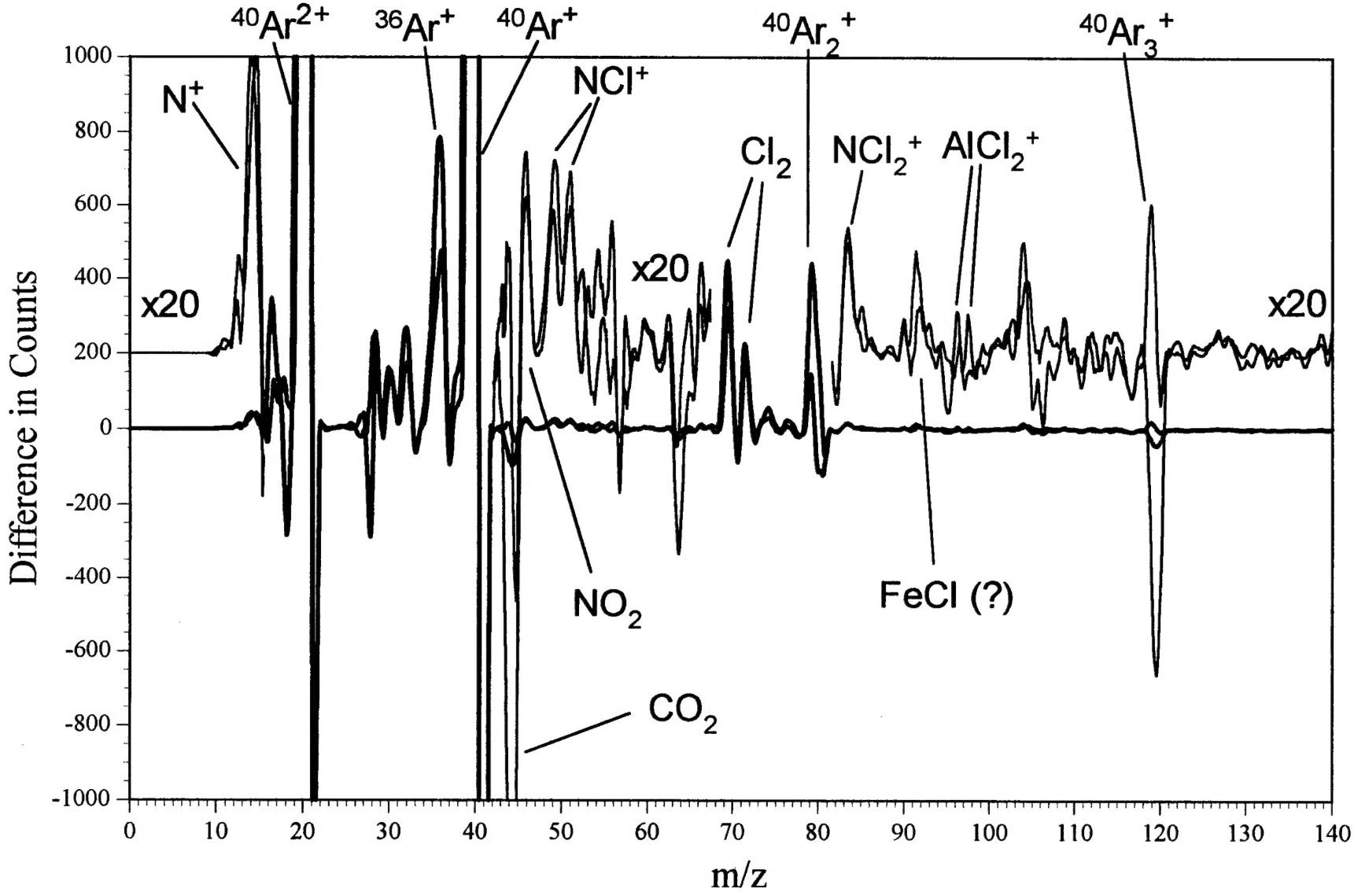


Figure 7 - Supersonic pulse, plasma sampling mass spectra showing the products of the chlorine etching of AlN. The spectra plotted are the of subtracting a background spectrum taken before chlorine gas flow was initiated.

6. List of Publications

8 S.F. Webb, G.A. Gaddy and Rik Blumenthal, "Investigation of ECR-microwave Plasmas Using Methane as the Hydrocarbon Source Gas," in preparation.

7 S.F. Webb, G.A. Gaddy and Rik Blumenthal, "Investigation of ECR-microwave Plasmas Using Ethane as the Hydrocarbon Source Gas," to be submitted to **Journal of Vacuum Science and Technology A.**

6 G.A. Gaddy, S.F. Webb and Rik Blumenthal, "Supersonic Pulse, Plasma Sampling Mass Spectrometry: Theory and Practice," **Plasma Chemistry and Plasma Processing, in press.**

5 S.F. Webb, G.A. Gaddy and Rik Blumenthal, "Distribution of species within an ethylene ECR-microwave plasma," **Journal of Vacuum Science and Technology A 16**(4)(1998),2148-2152

4 G.A. Gaddy, S.F. Webb and Rik Blumenthal, "Mass spectrometric determination of the percent dissociation of a high-density chlorine plasma," **Applied Physics Letters** 71(22) (1997), 3206-3208.

3 Rik Blumenthal, "Chemical reactions responsible for the plasma etching of silicon" Proceedings of the 28th Plasmadynamics and Lasers Conference, American Institute of Aeronautics and Astronautics, Restin VA, Paper Number: AIAA-97-2403.

2 S.F. Webb, G.A. Gaddy and Rik Blumenthal, "Determining the number of chemical steps responsible for the distribution of chemical species in an ECR microwave plasma," **Journal of Vacuum Science and Technology A** 15(3) (1997), 647-653.

1 H. Hzu, S.F. Webb and Rik Blumenthal, "The Chemical Composition of Diamond Plasmas" **Journal of Vacuum Science and Technology A** 14(3) (1996), 952-959.

7. List of Participating Scientific Personnel

Rik Blumenthal, Ph.D., Assistant Professor of Chemistry
Hongbin Zhu, Graduate Student, no degree awarded, transferred to another department
Sharon F. Webb, Graduate Student, no degree awarded as of reporting date
Gregory A. Gaddy, Graduate Student, no degree awarded as of reporting date

8. Report of Inventions None.

9.Bibliography

---


1 I.P Herman, "*Optical diagnostics for thin film processing*" (Academic Press, San Diego, 1996).

2 W.L. Hsu, J. Appl. Phys. **72**, 3102 (1992).

3 D. Leonhardt, C. R. Eddy Jr., V. A. Shamamian, R. T. Holm, O. J. Glembocki, and J. E. Butler, J. Vac. Sci. Technol. A **16(3)**, 1547 (1998).

4 For instance, the Hiden EQP Plasma Probe

5 J.B. Anderson, in *Molecular Beams and Low Density Gas Dynamics*, edited by P.P. Wegener (Marcel Dekker, New York, 1974) pp 1-92.

6 O.F. Hagena, ibid, pp 94-181.

7 S.B. Rayali and J.B. Fenn, Ber. Bunsenges. Phys. Chem., **88**, 245 (1984).

8 G.A. Cook, "*Argon, Helium and the Rare Gases, The Elements of the Helium Group*" (Interscience, New York, 1961).

9 J.P. Hirth, in *Progress in Materials Science: Condensation and Evaporation, Nucleation and Growth Kinetics*, edited by B. Chalmers (MacMillan, New York, 1963).

10 See any textbook on Physical Chemistry, such as P.W. Atkins, "*Physical Chemistry - fifth ed.*" (Freeman, New York, 1994)

11 Bachmann, P.K., Leers, D. and Lydtin, H., **Diamond Rel. Materials, 1**,1 (1991).

12 H. Zhu, S.F. Webb, and R. Blumenthal, J. Vac. Sci. Technol. A **14(3)**, 952 (1996).

13 The approximately 5% ethane observed in the plasma spectrum is assigned to an ethane impurity in the acetylene feed gas. This same impurity is also observed in the plasma off (simple gas flow) spectra.

14 S.F. Webb, G.A. Gaddy and R. Blumenthal, J. Vac. Sci. Technol. A **15(3)**,647 (1997).

15 S.F. Webb, G.A. Gaddy and R. Blumenthal, J. Vac. Sci. Technol. A **16(4),** 2148 (1998).

16 S.F. Webb, G.A. Gaddy and R. Blumenthal, to be submitted to J. Vac. Sci. Technol. A.

17 J. Warnatz, in Combustion Chemistry, edited by W.C. Gardner (Springer-Velag, New York, 1984).

18 G.A. Gaddy, S.F. Webb and R. Blumenthal, Appl. Phys. Lett. **71(22)**, 3206 (1997).

19 Rik Blumenthal, in "*Proceedings of the 28th Plasmadynamics and Lasers Conference, American Institute of Aeronautics and Astronautics*" (AIAA, Restin VA, 1997) Paper Number: AIAA-97-2403.